SCIENTIFIC REPORTS

OPEN

SUBJECT AREAS:
CHEMICAL SYNTHESIS
BIOMARKER RESEARCH

Received
24 September 2013

Accepted
6 November 2013

Published
22 November 2013

Correspondence and requests for materials should be addressed to M.E. (mahmoud.elsabahy@chem.tamu.edu) or K.L.W. (wooley@chem.tamu.edu)

* These authors contributed equally to this work.

Surface Charges and Shell Crosslinks Each Play Significant Roles in Mediating Degradation, Biofouling, Cytotoxicity and Immunotoxicity for Polyphosphoester-based Nanoparticles

Mahmoud Elsabahy[1,2]*, Shiyi Zhang[1,3,4]*, Fuwu Zhang[1], Zhou J. Deng[3,4], Young H. Lim[1], Hai Wang[1], Perouza Parsamian[1], Paula T. Hammond[3,4] & Karen L. Wooley[1]

[1]Department of Chemistry, Department of Chemical Engineering, Laboratory for Synthetic-Biologic Interactions, Texas A&M University, P.O. Box 30012, 3255 TAMU, College Station, Texas 77842-3012, United States, [2]Department of Pharmaceutics, Faculty of Pharmacy, Assiut Clinical Center of Nanomedicine, Al-Rajhy Liver Hospital, Assiut University, Assiut, Egypt, [3]David H. Koch Institute for Integrative, Cancer Research, [4]Department of Chemical Engineering, Massachusetts Institute of Technology, Cambridge, MA 02139.

The construction of nanostructures from biodegradable precursors and shell/core crosslinking have been pursued as strategies to solve the problems of toxicity and limited stability, respectively. Polyphosphoester (PPE)-based micelles and crosslinked nanoparticles with non-ionic, anionic, cationic, and zwitterionic surface characteristics for potential packaging and delivery of therapeutic and diagnostic agents, were constructed using a quick and efficient synthetic strategy, and importantly, demonstrated remarkable differences in terms of cytotoxicity, immunotoxicity, and biofouling properties, as a function of their surface characteristics and also with dependence on crosslinking throughout the shell layers. For instance, crosslinking of zwitterionic micelles significantly reduced the immunotoxicity, as evidenced from the absence of secretions of any of the 23 measured cytokines from RAW 264.7 mouse macrophages treated with the nanoparticles. The micelles and their crosslinked analogs demonstrated lower cytotoxicity than several commercially-available vehicles, and their degradation products were not cytotoxic to cells at the range of the tested concentrations. PPE-nanoparticles are expected to have broad implications in clinical nanomedicine as alternative vehicles to those involved in several of the currently available medications.

Polymeric nanoparticles have demonstrated high efficiency in the delivery of various drugs (*e.g.* chemotherapeutics, nucleic acids and antimicrobial drugs) and several of them are currently in the market, under clinical trials or still in the laboratory research stage undergoing rigorous *in vitro* and *in vivo* investigations[1–4]. Among the many challenges towards clinical utilization of these nanoparticulates, two significant barriers to overcome are induction of various adverse biological reactions (*i.e.* toxicity, hypersensitivity, thrombosis, immunomodulatory effects, *etc.*) and destabilization before reaching their target sites or tissues[5,6]. The construction of nanostructures from degradable precursors and shell/core crosslinking has been pursued as strategies to solve the problems of toxicity and limited stability, respectively. Designing degradable nanomaterials is currently receiving great impetus due to their ability to degrade after delivering their therapeutic cargoes. In addition, the degradation rate might be tuned *via* incorporating various functionalities to control the degradation and/or to respond to a particular enzyme or pH, and hence allowing for controlled or stimuli-responsive drug delivery applications[7,8]. Although it is well known that nanoparticle surface charge influences their toxicities, this study reveals a delicate balance between nanoparticle composition, surface charge and stability on their biological responses.

Interactions between nanoparticles and the various components of the immune system can result in immunomodulatory effects, hence, avoiding recognition by the immune system is a straightforward strategy to overcome nanoparticle-induced toxicity[9]. The structure, composition, shape and surface chemistries of nanomaterials

dictate the type and extent of their interactions with the immune system components and thus the resulting immune response[9,10]. Evaluation of the immunotoxicity of nanomaterials, partially, by measuring the levels of cytokines, in particular the proinflammatory cytokines, can be a useful tool in evaluating nanoparticle immunotoxicity[9]. High levels of cytokines upon treatment with nanoparticles are usually associated with toxicity, adverse reactions and low therapeutic efficacy[9,11]. Crosslinking of one or more of the compartments of the polymeric nanomaterials forms robust structures that have lower tendency of dissociation and aggregation than their micellar analogs and also allows to control the release rates of cargos[12]. In addition, the presence of stabilizing crosslinks has been shown recently to induce lower toxicity and immunotoxicity, as compared to their micellar counterparts, eventually due to limiting the release of free polymeric units and reducing the interactions with the surrounding cells and biomacromolecules[13,14].

Rapid and efficient synthesis and construction of nanomaterials are major concerns for translation into clinically-viable products[15,16]. Recently, we have developed an efficient and rapid synthetic strategy to program a series of polyphosphoester (PPE)-based micelles with various surface charges[17,18]. In this study, the effects of shell-crosslinking and surface charges on the degradation rate, protein adsorption and toxicity profiles of the neutral, anionic, cationic and zwitterionic micelles were studied. PPE-micelles and crosslinked nanoparticles were constructed *via* a rapid and efficient strategy that yielded nanosized particles with narrow size distributions, and versatile structures and surface chemistries. These nanoparticles demonstrated remarkable safety profiles and, hence, they are expected to have broad implications in clinical nanomedicine as alternative vehicles to those involved in several of the currently available medications.

Results

Polyphosphoester nanoparticles: self-assembly and shell crosslinking. PPE-based nanoparticles with different surface charges and shell-crosslinking extents were constructed, and their degradation kinetics and immunotoxicities were studied. Recently, we have developed a synthetic strategy to program a series of diverse, functional micelles with various surface charges from reactive monomers, in which all three steps are rapid, quantitative and conducted under mild conditions[17,19]. The hydrophobic-functional AB diblock PPE, poly(2-ethylbutyl phospholane)-*block*-poly(butynyl phospholane) (PEBP-*b*-PBYP) was synthesized by an ultrafast (<5 min) organocatalyzed ring-opening polymerization in a one-pot manner and was transformed into four amphiphilic diblock copolymers with different charges by "click" type thiol-yne reactions, which were then assembled into polymer micelles by direct dissolution into water[20]. In this study, those four types of polymeric micelles with different surface charges/functionalities, **1**–**4**, were constructed *via* self-assembly of non-ionic, anionic, cationic and zwitterionic diblock copolymers, and then the anionic, cationic and zwitterionic micelles (**2**–**4**) were further transformed through shell crosslinking reactions into stable shell-crosslinked knedel-like nanoparticles (SCKs, **5**–**7**), as shown in Figure 1.

Four micelles were self-assembled from four amphiphilic diblock copolymers while three SCKs were constructed by shell crosslinking of the three charged micelles that possessed functionalities through which the crosslinking reactions could be performed. All four amphiphilic diblock PPEs were dissolved in nanopure water by sonication for 5 min and spontaneously formed spherical micelles, **1**, **2**, **3** and **4**, with narrow size distributions (see previous publication[17] for the characterization data). Three charged micelles were shell-crosslinked with different reagents *via* amidation reactions. To form the anionic SCKs, **5**, the carboxylic acid groups on the hydrophilic segment of diblock copolymer, which were located in shell domains of the anionic micelles, **2**, were activated by 1-[3′-(dimethylamino)propyl]-3-ethylcarbodiimide methiodide (EDCI) to react with the diamine compound, 2,2′-(ethylenedioxy)bis(ethylamine). This same strategy was applied to the construction of cationic SCKs, **6**, by coupling of the di-acid compound, Bis-dPEG®2-acid with amino groups in the shell domains of the cationic micelles, **3**, facilitated by the addition of EDCI. Since the shell domain of the zwitterionic micelle, **4**, contained both amino groups and carboxylic acid groups, EDCI was used to activate their coupling without using additional reagents in the construction of the zwitterionic SCKs, **7**. Due to the unavailability of chemical functionalities in the shell domain of the non-ionic micelle, **1**, preparation of a shell-crosslinked form of the non-ionic nanoparticle was not feasible. After the nominal 30% shell-crosslinking, SCK solutions were purified by extensive dialysis against nanopure water in the cold room to remove small compounds.

The sizes and size distributions of the three SCKs were characterized by both transmission electron microscopy (TEM) and dynamic light scattering (DLS), as shown in Figure 2. The circularly-shaped images observed by TEM suggested that these nanoparticles maintained micellar structure after the shell crosslinking. TEM images of **5**, **6**, and **7** showed uniform nanoparticles with average sizes of approximately 16, 16 and 23 nm, respectively (Figures 2a, 2c, 2e). DLS results showed narrow and mono-modal size distributions of nanoparticles in all three SCKs. The number-averaged hydrodynamic diameters (D_h(number)) of **5**, **6** and **7** were 16 ± 4 nm, 15 ± 3 nm and 23 ± 6 nm, respectively (Figures 2b, 2d, 2f). The maintenance of the SCK dimensions with their corresponding micelles indicated that inter-particle crosslinking was not prevalent during the intra-particle crosslinking process. By shell-crosslinking, three charged micelles were transferred into three robust SCKs without changing their sizes or size distributions.

The zeta-potential values were measured for the four micelles and three SCKs in buffer solutions at pH 5.0 and pH 7.4 by Delsa Nano C particle analyzer (Figure 3). The non-ionic micelle, **1**, had slightly negative zeta potentials of −12.2 mV at pH 7.4 and −18.0 mV at pH 5.0. The negative-charged nature of the anionic micelles, **2**, and anionic SCKs, **5**, was confirmed through zeta potential measurements. After the shell crosslinking, **5** maintained low zeta potentials, −34.7 mV at pH 7.4 and −28.4 mV at pH 5.0, which were slightly higher than those of **2** due to the partial consumption of carboxylic acid groups during the shell crosslinking process. Similarly, the cationic SCKs, **6**, sustained the positive zeta potentials at both pH 7.4 and pH 5.0, but to a lesser extent, as compared to the cationic micelles **3**, due to the consumption of some amino groups for the shell crosslinking. Since the shell crosslinking of zwitterionic micelles consumed both the carboxylic and amino groups, the resulting zwitterionic SCKs, **7**, had zeta potentials at both pH 7.4 and pH 5.0 that were similar to their micellar analogs **4**. The zeta potential measurements confirmed the expected surface charges and surface functionalities of the four micelles and three SCKs.

Effect of pH, surface chemistry and crosslinking on degradation profiles of PPE-nanoparticles. PPE nanoparticles are attractive for biomedical applications mainly because of their biodegradability and chemical compositional versatility, which was expected to allow for tuning of their rates of degradation and the accommodation of drugs having various structures, solubilities and sizes. These nanoparticles undergo degradation either by spontaneous hydrolysis or in the presence of certain enzymes, due to the cleavage of their phosphodiester backbones and phosphoester side chains. Penczek and coworkers first investigated the hydrolytic degradation kinetics of poly(methyl ethylene phosphate) and poly(trimethylene phosphate) by direct titrimetric and NMR methods[21]. They found that the hydrolysis rates of the polymers were comparable to those of small molecule model compounds, and were strongly dependent on pH; increasing more than 100 times between acidic (pH = 1)/basic

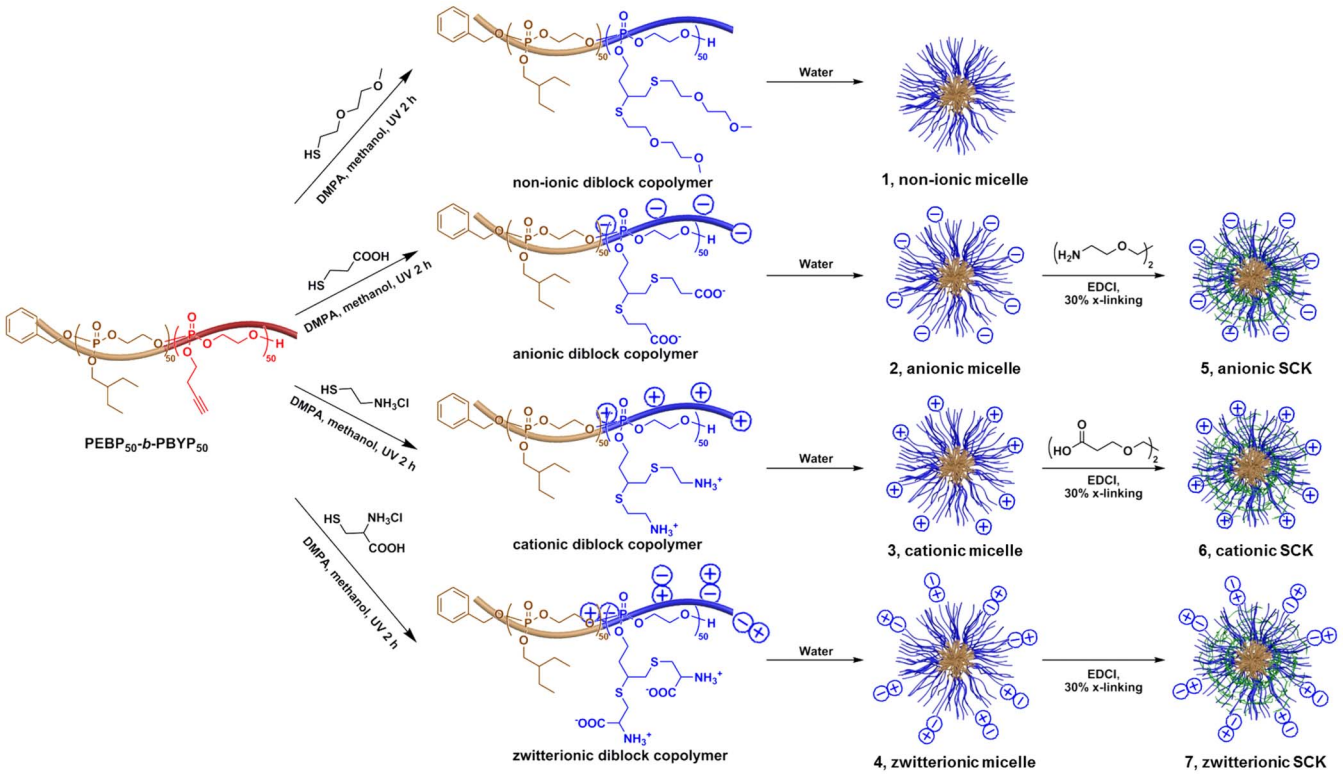

Figure 1 | **Schematic representation of the self-assembly of four amphiphilic diblock copolymers into non-ionic micelle (1), anionic micelle (2), cationic micelle (3) and zwitterionic micelle (4), and the shell-crosslinking of resulting three charged micelle into anionic SCKs (5), cationic SCKs (6) and zwitterionic SCKs (7).** Adapted and modified with permission from reference[17]. Copyright (2013) American Chemical Society.

(pH = 13) and neutral (pH = 7) conditions. The results from several other groups also demonstrated that PPE-based nanoparticles[22–24] and hydrogels[25–28] were relatively stable in neutral conditions for dozens of days and up to several months, and accelerated degradations in acidic and basic conditions were noted, as monitored by gel permeation chromatography (GPC) and NMR spectroscopy. The hydrolytic degradation rates were controllable by adjusting the chemical structure in the backbone or side chain, for instance, amino group-containing cationic PPEs degraded at accelerated rates[29,30]. The hydrolytic degradation products exhibited good

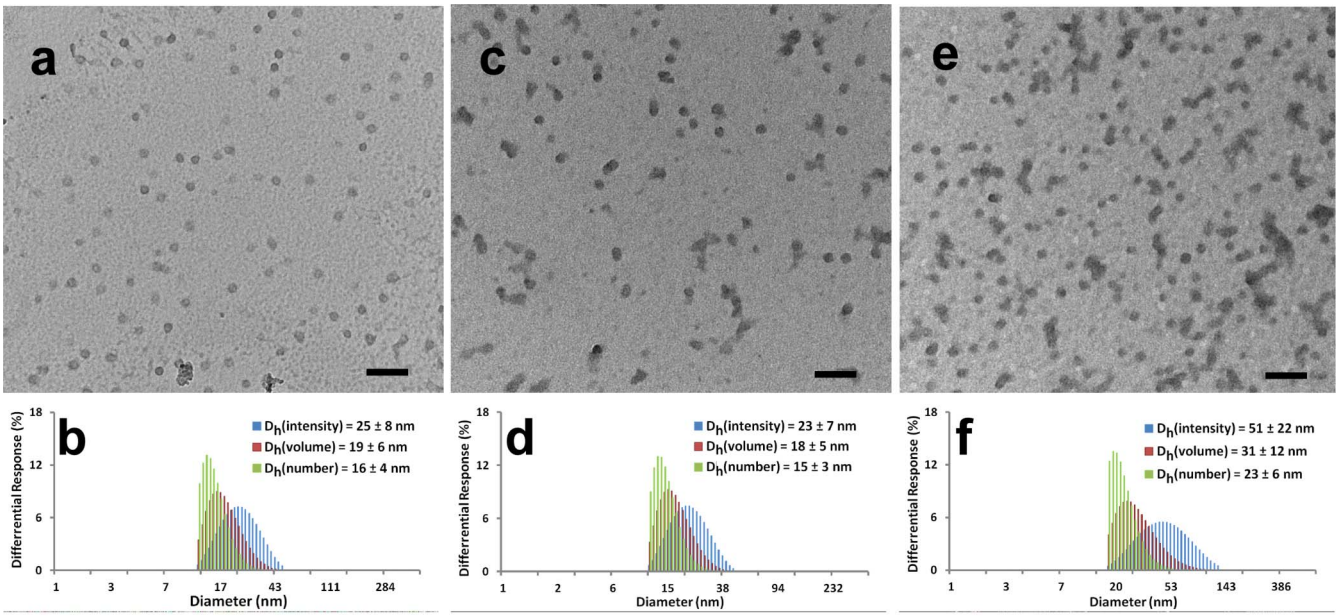

Figure 2 | (a), TEM image of **5**, average diameter is 16 ± 3 nm, after counting more than 100 particles. (b), DLS results of **5**: D_h(intensity) = 25 ± 8 nm, D_h(volume) = 19 ± 6 nm, D_h(number) = 16 ± 4 nm, PDI = 0.06. (c), TEM image of **6**, average diameter is 16 ± 4 nm, after counting more than 100 particles. (d), DLS results of **6**: D_h(intensity) = 23 ± 7 nm, D_h(volume) = 18 ± 5 nm, D_h(number) = 15 ± 3 nm, PDI = 0.04. (e), TEM image of **6**, average diameter is 21 ± 5 nm, after counting more than 100 particles. (f), DLS results of **7**: D_h(intensity) = 55 ±22 nm, D_h(volume) = 31 ± 12 nm, D_h(number) = 23 ± 6 nm, PDI = 0.07. All scale bars in TEM images are 100 nm.

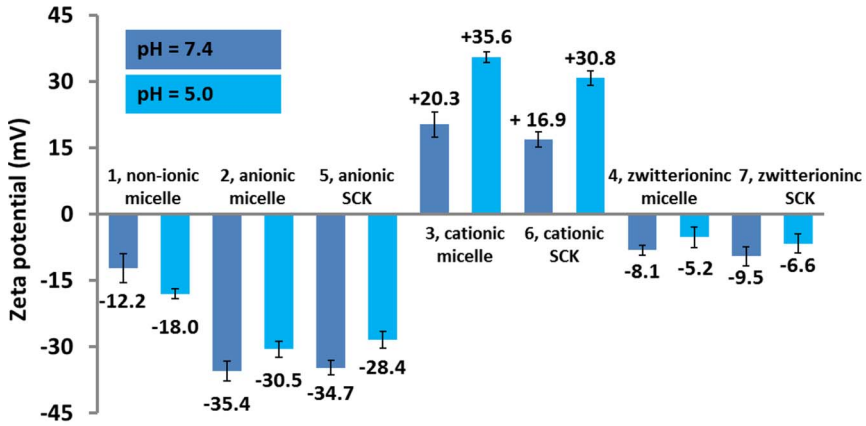

Figure 3 | Zeta potential values of micelles 1, 2, 3, 4 and SCKs 5, 6, 7 in PBS buffer solutions at pH 7.4 and pH 5.0. The average values and their standard deviations, from six measurements, are shown.

biocompatibility to several cell lines[24,26–28]. Since PPE nanoparticles share the structural similarity of some naturally-existing polymers (*e.g.* nucleic and teichoic acids), and phosphoester bonds are widely represented in living systems, researchers are actively looking for enzymes for the specific and accelerated degradation of PPE-based materials. Minor degradation of PPE nanoparticles was observed in the presence of *Pseudomonas* lipase for 24 h, after the degradation of the poly(ε-caprolactone) (PCL) segment of PCL-*b*-PPE copolymers, monitored by GPC[31,32]. Phosphoester-specific enzymes (*e.g.* alkaline phosphatase) were found to accelerate the degradation of PPE-based hydrogels at pH 9.0[33]. Phosphodiesterase I also promoted the degradation of PPE-based micelles/nanogels at pH 8.8[32,34], and expedited the release of drug encapsulated in the nanoparticles[35–37].

To investigate the hydrolytic degradation of PPE-based nanoparticles with different surface charges and shell-crosslinking extent under physiological conditions, we monitored the sizes and surface charges of nanoparticles during the degradation when incubated in pH 7.4 and pH 5.0 buffers at 37°C. Compared with literature reported degradation data, this study employed DLS and zeta potential analyses to monitor the changes in the overall nanoparticle structures and properties that were expected to influence their overall biological interactions, instead of using NMR and GPC to track the breakage of bonds. pH 7.4 stands for physiological environments, while pH 5.0 is a typical pH that is commonly utilized to study the behavior of nanoparticles to mimic the pH of endosomes/lysosomes and the acidic pH of tumor tissues.

The non-ionic micelle, **1**, had similar degradation profiles in pH 7.4 and pH 5.0 buffers, as shown in Figure S1. Non-ionic micelles maintained their sizes at both pHs for about 4 weeks with a slight decrease of zeta potential values. The sizes of micelles became smaller, until reaching 3 nm and then became undetectable by DLS, while the charges of the micelles became more negative until −40 mV. This trend of becoming more negatively charged may be due to the simultaneous hydrolysis of phosphoester linkages in the main chain and the side chain that yielded negatively-charged phosphate groups.

Anionic micelles, **2**, and anionic SCKs, **5**, had different degradation profiles in terms of particle sizes, but maintained similar charges during the degradation study (Figure S2). Both at pH 7.4 and pH 5.0 buffers, the zeta potentials of anionic micelles and anionic SCKs slowly dropped to around −45 mV over the period of 18 weeks. The anionic SCKs maintained their sizes for 10 weeks, and then became smaller to 3 nm until becoming undetectable by DLS. In contrast, the anionic micelles could maintain their sizes for only 4 weeks in pH 7.4 buffer and for 6 weeks at pH 5.0. This difference may result from crosslinking the shell domains of micelles, which formed structures of higher stability[7]. For both anionic micelles and SCKs, the sizes decreased more gradually in pH 5.0 buffer than in pH 7.4 buffer.

Cationic micelles, **3**, and cationic SCKs, **6**, degraded much faster than did the other nanoparticles. After 10 days of degradation, in both pH 5.0 and pH 7.4 buffers, no particles could be observed by TEM, and a signal was barely detected by DLS. The zeta potentials of both micelles and SCKs transitioned from positive to neutral, and finally reached a negative value of *ca.* −35 mV (Figure S3). This trend may be due to the loss of cationic side groups upon hydrolysis. Both cationic micelles and cationic SCKs reached neutrality at pH 7.4 one day earlier than at pH 5.0. This difference may result from intramolecular attack of the phosphoester bonds by deprotonated amino groups. Hydrodynamic diameters of SCKs had a tendency of getting smaller until becoming undetectable by DLS, except for the formation of large aggregates at the isoelectric points, where zeta potentials were almost zero. For the degradation of micelles, large aggregates formed at the isoelectric points, but did not disappear until the late stage. This difference may be explained by cationic micelles undergoing re-assembly during the degradation, whereas cationic SCKs maintained the micellar structures because of the crosslinking of the shell domain[38]. The degradation study demonstrated that PPE-based cationic nanoparticles degraded in days and lost the cationic feature rapidly.

The degradation rates of zwitterionic nanoparticles, which maintained their sizes for 2–4 weeks, were between those of anionic and cationic nanoparticles (Figure S4). The degradation of PPE-based nanoparticles is due to the cleavage of phosphoester linkages. In pH 7.4 and pH 5.0 buffers, the phosphorus atom may be attacked by nucleophiles, like hydroxide or amine. More deprotonated amine groups on the nanoparticles would result in faster degradation rate.

The degradation studies of non-ionic, anionic, cationic and zwitterionic micelles and SCKs demonstrated the higher stability of SCKs. For the PPE-based nanoparticles, the one with amine groups degraded much faster than did the others. Anionic and zwitterionic nanoparticles would be stable in buffers for several weeks without dramatic changes in nanoparticle sizes. The zeta potentials of all nanoparticles decreased to −35 to −45 mV in the time windows of their degradation profiles, days for cationic nanoparticles while weeks for non-ionic, anionic and zwitterionic nanoparticles, indicating the formation of negatively-charged phosphates in place of the phosphoester backbone and side chain linkages. In general, the hydrolytic degradation was slightly faster in pH 7.4 buffer than in pH 5.0 buffer.

Cytotoxicity of PPE-nanoparticles and their degradation products. Because of the broad ranges of chemical compositions and

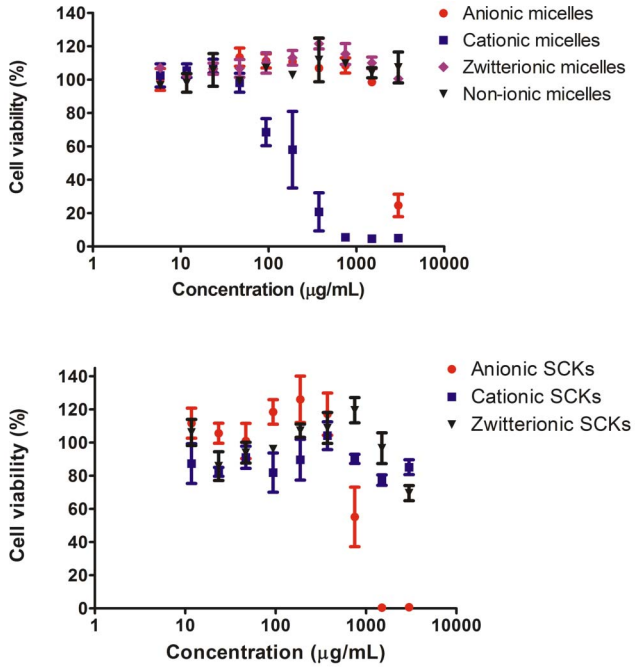

Figure 4 | Viability of cells (%) treated with non-ionic-, zwitterionic-, cationic-, anionic-PPE micelles, zwitterionic-, cationic- and anionic-PPE SCKs. The values are presented as mean ± SD of at least triplicates. The graphs that present Lipofectamine, PEI, Cremophor-EL, the degradation products of the various PPE-based nanoparticles and various combinations of nanoparticles are in the Supporting Information (Figure S5).

potential biomedical applications that are available for PPE-based nanoparticulate micelles and SCKs, it was important to determine their cytotoxicities and immunotoxicities, with comparisons being made against commercially available vehicles. Therefore, the viabilities and induced cytokine levels of RAW 264.7 mouse macrophages were measured following 24 h incubation with increasing concentrations of the series of neutral, anionic, cationic, and zwitterionic PPE micelles and SCKs, and also against Lipofectamine, polyethyleneimine (PEI), and Cremophor-EL, with comparisons to the control-untreated cells (Figure 4, Figure S5 and Table 1). In addition, the degradation products of the entire series of PPE-nanoparticles (both micelles and SCKs) were prepared by incubation in phosphate-buffered saline (PBS) at pH 7.4 and 37°C, with continuous shaking for 20 weeks under aseptic conditions. After complete degradation of the nanoparticles (until no nanoparticles could be detected by dynamic light scattering measurements), the solutions were lyophilized into powders before being tested for their cytotoxicities and immunotoxicities. Lipofectamine, PEI and Cremophor-EL were selected as examples of cationic (Lipofectamine and PEI) and non-ionic (Cremophor-EL) vehicles that are commonly utilized for the delivery of nucleic acids and hydrophobic drugs, respectively.

In general, the neutral (*i.e.* non-ionic) and zwitterionic PPE-based micelles and SCKs were less cytotoxic than Lipofectamine, PEI and Cremophor-EL (Table 1). For the anionic PPE-micelles, toxicity was observed at high concentrations (3000 μg/mL). Surprisingly, the cytotoxicity was enhanced upon crosslinking the anionic micelles. This effect might be due to the higher stability of SCKs against degradation (See Figure S2). Because the degradation products of both the anionic micelles and SCKs have limited toxicity, the faster degradation of micelles into the less-cytotoxic degradation products might explain the lower cytotoxicity of the parent micelles as compared to the parent SCKs. We have previously reported that PPE-based cationic micelles had 6-fold lower cytotoxicity than Lipofectamine[17]. In this study, PPE-cationic micelles were found to have 42-fold lower cytotoxicity than PEI. Interestingly, crosslinking of the PPE-cationic micelles yielded SCKs that were not cytotoxic up to a concentration of 3000 μg/mL.

The degradation products of neutral, anionic, cationic and zwitterionic micelles and their crosslinked nanoparticle analogs did not show any toxicity to cells up to a concentration of 3000 μg/mL, which is an indication that the released products after degradation do not have a considerable toxicity to cells. In a previous study, hydrolytic degradation products of monomethyl ether poly(ethylene glycol) (mPEG)-*b*-poly(ethyl ethylene phosphate) micelles were not toxic to cells up to a concentration of 500 μg/mL[24]. The PPE nanoparticles developed in the current study can be rapidly synthesized and provide versatile nanostructures (anionic, neutral, cationic or zwitterionic), with control over their surface chemistries to accommodate and deliver anionic, cationic, and/or hydrophobic guest (macro)molecules. In addition, the cytotoxicity data reveal that PPE-based nanoparticulates may have a remarkable safety profile, as compared to commercially-available vectors, and degradable/non-degradable nanoparticles developed previously by our group[39,40], and by others[41,42].

Anti-biofouling properties of PPE-nanoparticles. The anti-biofouling properties of the series of PPE-micelles and SCKs were studied. Briefly, nanoparticles were incubated with a fixed amount of 23 different cytokines, and the apparent concentrations of cytokines were measured using a multiplex assay and compared to a solution treated in the same way but containing no nanoparticles. The lower the apparent measured concentration of free cytokines in the supernatant, the higher the adsorption competencies of the nanoparticles. The adsorption of cytokines was qualitatively assessed by calculating the *p* values, which imply the statistical significance of differences between the treatments and the controls (Table 2). Although adsorption of cytokines on nanoparticles has been observed previously[43,44], it is also possible that nanoparticles may interfere with some of the multiplex assay components (antibodies, beads, *etc.*). The 23 measured cytokines were interleukin (IL)-1α, IL-1β, IL-2, IL-3, IL-4, IL-5, IL-6, IL-9, IL-10, IL-12 (P40), IL-12 (P70), IL-13, IL-17, Eotaxin, granulocyte-colony-stimulating factor (G-CSF), granulocyte macrophage-colony-stimulating factor (GM-CSF), interferon-γ (IFN-γ), keratinocyte-derived chemokine (KC), monocyte chemotactic protein (MCP)-1, macrophage inflammatory protein (MIP)-1α, MIP-1β, regulated upon activation normal T-cell expressed and presumably secreted (RANTES) and tumor necrosis factor-α (TNF-α).

Zwitterionic micelles and SCKs had the least adsorption of the cytokines, a phenomenon that is in agreement with literature reports[45–47]. The zwitterionic characteristic of nanoparticles is hypothesized to impart anti-biofouling properties by electrostatically binding water molecules more tightly than the hydrogen bonding of water in the case of PEG and, thus, resulting in higher hydration of the corona, which is critical in minimizing protein adsorption and generating stealth properties[48]. However, we have reported recently that zwitterionic poly(carboxybetaine) polymeric coating resulted in higher adsorption of cytokines, when compared to PEG, when both PEG and poly(carboxybetaine) were grafted onto poly(acrylic acid)-*b*-poly($_{D,L}$-lactide)-SCKs[49]. Hence, it seems that protein adsorption and interactions between nanomaterials and biomolecules in the surrounding environment depend not only on the polymeric coating, although a critical factor, but also on other characteristics of nanoparticles (composition, size, zeta-potential, presence/absence of crosslinks, type of core materials, *etc.*). The neutral micelles adsorbed low amounts of cytokines. Both anionic and cationic micelles and SCKs adsorbed more cytokines than did the zwitterionic nanoparticles. In particular, the cationic nanoparticles were associated with higher protein adsorption, as compared to the anionic analogs. The

Table 1 | The cytotoxicity (IC_{50}) of PPE-based micelles and SCKs, and some commonly utilized delivery vehicles, such as, Lipofectamine, PEI and Cremophor-EL in RAW 264.7 mouse macrophages. The cytotoxicity of the degradation products of PPE-nanoparticles and their PEBP-*b*-PBYP backbone are also included. Values are presented as mean ± SD of at least triplicates

Controls	IC_{50} (μg/mL) ± SD	PPE-Micelles	IC_{50} (μg/mL) ± SD	PPE-SCKs	IC_{50} (μg/mL) ± SD	PPE-Deg	IC_{50} (μg/mL) ± SD
Lipofectamine	31.4 ± 6	Anionic micelles	1705 ± 16	Anionic SCKs	761 ± 38	Anionic micelles-Deg	*
PEI	4.3 ± 1	Cationic micelles	180 ± 48	Cationic SCKs	*	Cationic micelles-Deg	*
Cremophor-EL	1700 ± 113	Zwitterionic micelles	*	Zwitterionic SCKs	*	Zwitterionic micelles-Deg	*
		Non-ionic micelles	*			Non-ionic micelles-Deg	*
						Anionic SCKs-Deg	*
						Cationic SCKs-Deg	*
						Zwitterionic SCKs-Deg	*
						PEBP-*b*-PBYP-Deg	*

*The IC_{50} values could not be determined because high cell-viabilities were observed over the range of the tested concentrations, up to 3000 μg/mL.

cationic carriers are known to have higher capacity for interactions with cells, proteins and biomolecules than neutral and anionic nanoparticles. For instance, Deng *et al.* have demonstrated that modification of the surface charge of polymer-coated gold nanoparticles had a great influence on the protein adsorption competences of the nanoparticles. Consistent with our results, they found that neutral nanoparticles had lower affinity for protein adsorption than did anionic and cationic nanoparticles[50].

Immunotoxicities of PPE-micelles and SCKs, and their degradation products. Proinflammatory cytokines (*e.g.* IL-1, IL-6 and TNF-α) serve as mediators of inflammatory and immunologic reactions and activate functions of several inflammatory cells during acute inflammatory responses[9,51]. The immunotoxicities of the PPE micelles, SCKs and their degradation products were studied by incubating RAW 264.7 mouse macrophages with the various formulations (5 μg/mL) for 24 h, followed by measuring the levels of 23 different cytokines using the previously established multiplexing assay (Figure 5 and Tables S1–S4)[49]. The *in vitro* immunotoxicity, evaluated by the number of induced cytokines, for PPE micelles was highest for cationic micelles (13 cytokines) and decreased according to zwitterionic (7 cytokines) > neutral (3 cytokines) > anionic micelles (1 cytokines). For the PPE SCKs, immunotoxicity was also higher for cationic SCKs (12 cytokines) than for anionic SCKs (3 cytokines), whereas the zwitterionic SCKs did not induce the secretions of any of the tested cytokines. These proinflammatory cytokines have been well studied and characterized as participants in the basic inflammatory process and mediators of cellular infiltration[52–57]. Degradation products of PPE-micelles and SCKs induced minimal release of the tested cytokines. A similar pattern was observed for the degradation products of the PEBP-*b*-PBYP backbone. Among all the tested formulations and their degradation products, the three nanoparticles which induced the release of most of the tested cytokines were cationic micelles and SCKs and zwitterionic micelles. It is known that cationic carriers interact rapidly and strongly with the membranes of cells and are endocytosed to greater extents than are neutral or anionic carriers. Surprisingly, zwitterionic micelles induced high release of the tested cytokines (7 cytokines, Figure 5 and Table S3). Neutral micelles also induced the release of several cytokines (Table S4). Remarkably, the induction of cytokines was substantially reduced simply by the introduction of crosslinks within the shells of the zwitterionic micelles.

It has been reported previously that crosslinking can reduce the cytotoxicity and immunotoxicity of polymeric micelle assemblies[13,14]. Crosslinking of cationic micelles reduced their immunotoxicity (Table S2). Furthermore, crosslinking of zwitterionic micelles significantly reduced the immunotoxicity of the PPE-nanoparticles (Table S3). However, there is an observed increase in cytotoxicity and immunotoxicity upon crosslinking anionic PPE-micelles (Table S1). This effect might be due to the higher stability of the SCKs against degradation (See Figure S2). Because the degradation products of both the anionic micelles and SCKs have limited immunotoxicity, the faster degradation of the micelles into the less-cytotoxic and -immunotoxic degradation products may explain the lower immunotoxicity of the parent micelles as compared to the parent SCKs. A similar trend was observed in terms of cytotoxicity (*vide supra*, IC_{50} values of 1705 ± 16 *vs.* 761 ± 38 for anionic micelles *vs.* anionic SCKs, respectively, Table 1).

Discussion

PPE-based micelles and crosslinked nanoparticles with various surface charges, which have been designed for a variety of biomedical applications (non-ionic, anionic, and zwitterionic surface characteristics for packaging and delivery of therapeutics to treat infectious diseases or cancer, and cationic for delivery of nucleic acids for the

Table 2 | Cytokines adsorption on anionic, cationic, neutral and zwitterionic micelles, and the anionic, cationic and zwitterionic SCKs. The adsorption of cytokines was calculated based on apparent concentrations of cytokines measured when incubated with nanoparticles, as compared to their concentrations in a solution treated in the same way but containing no nanoparticles. The indicated *p* values highlight the significance of differences between the measured concentrations of the treatment and the control, and only cytokines of *p* values less than 0.05 are shown in the table

Nanoparticles	Adsorbed cytokines	*p* value
Anionic micelles	IL-12(p40)	0.0002
	IL-17	0.002
	IFN-γ	0.03
Cationic micelles	IL-1α	0.000009
	IL-17	0.00002
	IL-4	0.00002
	MIP-1β	0.00007
	IL-2	0.00008
	KC	0.0002
	IL-12(p40)	0.0003
	IL-9	0.003
	IL-12(P70)	0.004
	IL-1β	0.005
	IL-3	0.01
	IFN-γ	0.02
	RANTES	0.02
	MIP-1α	0.04
Zwitterionic micelles		
Non-ionic micelles	MIP-1β	0.002
	IL-9	0.02
	RANTES	0.04
Anionic SCKs	IL-17	0.003
	IL-12(p40)	0.007
	Eotaxin	0.04
	IL-10	0.04
Cationic SCKs	IL-2	0.0002
	MIP-1β	0.0005
	IL-12(p40)	0.0007
	IL-9	0.0009
	KC	0.0009
	IL-1α	0.001
	IL-12(p70)	0.004
	RANTES	0.005
	IL-13	0.01
	IL-17	0.01
	Eotaxin	0.02
	IL-4	0.02
Zwitterionic SCKs	IL-12(p40)	0.001

treatment of inflammatory diseases or cancer)[8,18,58–60], were constructed using a quick and efficient synthetic strategy, and importantly, demonstrated remarkable differences in terms of cytotoxicity, immunotoxicity, and anti-biofouling properties, as a function of their surface charge characteristics and also with dependence on crosslinking throughout the shell layers. The micelles and their crosslinked analogs demonstrated lower cytotoxicity than several commercially-available vehicles, with crosslinking of the cationic micelles being highly efficient in further reducing the cytotoxicity of the micelles. The key conclusion from this study is that every nanoparticle should be rigorously investigated on individual basis and generalization can be seriously misleading, as the behavior of nanoparticles and their forming polymers differs significantly from one type of nanoparticle to another. In these particular PPE-based degradable nanoparticles, crosslinking has proven to play an important role in controlling stability, cytotoxicity and immunotoxicity of some of the characterized nanoparticles. In particular, zwitterionic micelles and SCKs and their degradation products exhibited exceptional safety profiles, with no cytotoxicity observed up to a concentration of 3000 μg/mL and without adsorbing any of the tested cytokines. In addition, crosslinking of zwitterionic micelles significantly reduced the immunotoxicity, as evidenced from the absence of secretions of any of the 23 cytokines, whereas the micellar counterpart induced the release of 7 cytokines from RAW 264.7 mouse macrophages treated with the nanoparticles. The degradation products of PPE-micelles and their crosslinked analogs were not cytotoxic and induced low immunotoxicity. These nanoparticles are currently being exploited for delivery of various therapeutics (*e.g.* nucleic acids and antimicrobial agents), and for administration *via* various routes, such as inhalational therapy. Moreover, with the convenient ability to tune the surface chemistry, these nanomaterials have the possibility of being expanded into highly complex hierarchically-assembled theranostics[40]. Future *in vitro* and *in vivo* characterizations of these nanoparticles and their utilization for delivery of various drugs, and decoration with targeting moieties will broaden their applications in clinical nanomedicine.

Methods

Details of experimental procedures and characterizations are included in the supporting information.

1. Self-assembly of functional diblock copolymers. The functional diblock copolymers (5.0 mg) were suspended into nanopure water (1.0 mL) and sonicated for 10 min.

The anionic diblock copolymers (30.0 mg, 0.100 mmol of acrylic acid) were suspended into ultrapure water (6.0 mL) and sonicated for 10 min. After being stirred for 1 h, a clear solution containing the anionic micelles was obtained. To a stirred solution of anionic micelle in a round-bottom flask equipped with a stir bar was added, dropwisely over 10 min, a solution of 2,2′-(ethylenedioxy)bis(ethylamine) (2.2 mg, 0.015 mmol) in ultrapure water (1.0 mL). The solution was allowed to stir for 1 h at room temperature. To this reaction mixture was added dropwisely, *via* a metering pump at the rate of 2 mL/h, a solution of EDCI (9.8 mg, 0.035 mmol) dissolved in ultrapure water (2 mL). The reaction mixture was allowed to stir overnight at room temperature and was then transferred to presoaked dialysis membrane tubes (MWCO *ca.* 6–8 kDa), and dialyzed against nanopure water for 36 h in the cold room (4–8°C) to remove small molecules. Final concentration of anionic SCK solution was adjusted to 2.5 mg/mL by the buffer solution to the desired pH or by ultrapure water. The anionic SCKs solution was lyophilized into powder and kept in the freezer (−20°C) for long term storage before being tested.

The cationic diblock copolymers (30.0 mg, 0.097 mmol of amino group) were suspended into ultrapure water (6.0 mL) and sonicated for 10 min. After being stirred for 1 h, a clear solution containing the cationic micelles was obtained. A solution of the diacid crosslinker (Bis-dPEG®2-acid, 3.0 mg, 0.015 mmol) in ultrapure water (1.0 mL) was added dropwisely to a stirred solution of micelle in a 5-mL vial. The mixture solution was allowed to stir for 1 h at room temperature. To this reaction mixture was added dropwisely, *via* a metering pump at the rate of 2 mL/h, a solution of EDCI (9.8 mg, 0.035 mmol) dissolved in ultrapure water (2 mL). The reaction mixture was allowed to stir overnight at room temperature and was then transferred to presoaked dialysis membrane tubes (MWCO *ca.* 6–8 kDa), and dialyzed against ultrapure water for 36 h in the cold room (4–8°C) to remove small molecules. Final concentration of cationic SCKs was adjusted to 2.5 mg/mL by the buffer solution to the desired pH or by ultrapure water. The cationic SCKs solution was lyophilized into powder and kept in the freeze (−20°C) for the long term storage and transportation before being tested.

The zwitterionic diblock copolymers (30.0 mg, 0.081 mmol of acrylic acid, 0.081 mmol of amino group) were suspended into ultrapure water (6.0 mL) and sonicated for 10 min. After being stirred for 1 h, a clear solution containing the zwitterionic micelles was obtained. To this micelle solution was added dropwisely a solution of EDCI (7.2 mg, 0.027 mmol) dissolved in ultrapure water (2 mL). The reaction mixture was allowed to stir overnight at room temperature and was then transferred to presoaked dialysis membrane tubes (MWCO *ca.* 6–8 kDa), and dialyzed against ultrapure water for 36 h in the cold room (4–8°C) to remove small molecules. Final concentration of zwitterionic SCKs was adjusted to 2.5 mg/mL by the buffer solution to the desired pH or by ultrapure water. The zwitterionic SCKs solution was lyophilized into powder and kept in the freeze (−20°C) for the long term storage and transportation before being tested.

2. Degradation studies. In a typical degradation experiment, a solution of nanoparticles (micelles or SCKs) was adjusted to pH 5.0 or pH 7.4 by 150 mM PBS buffer. The mixture solution was incubated in the 37°C shaker. The size, size distribution and zeta potential were measured by Delsa Nano C particle analyzer during the degradation.

For the cytotoxicity and immunotoxicity studies, a solution of nanoparticles (micelles or SCKs, 2.5 mg/mL, 8 mL) was adjusted to pH 7.4 by PBS buffer (12 mM, 2 mL, without NaCl or KCl) and incubated in a shaker at 37°C for 20 weeks. After

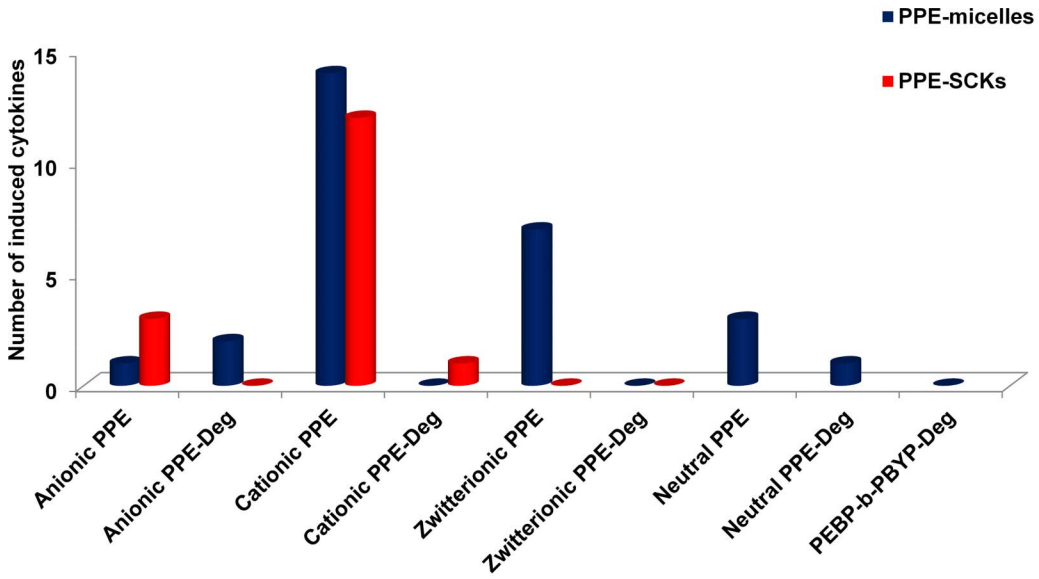

Figure 5 | The number of induced cytokines following treatment of RAW 264.7 mouse macrophages with PPE-micelles and SCKs of various surface charges (non-ionic, cationic, anionic and zwitterionic), and their degradation products at 5 μg/mL for 24 h. The 23 measured cytokines were IL-1α, IL-1β, IL-2, IL-3, IL-4, IL-5, IL-6, IL-9, IL-10, IL-12 (P40), IL-12 (P70), IL-13, IL-17, Eotaxin, G-CSF, GM-CSF, IFN-γ, KC, MCP-1, MIP-1α, MIP-1β, RANTES and TNF-α.

fully degradation of nanoparticles, the solutions were lyophilized into powder before being tested. For the degradation of PEBP-*b*-PBYP backbone, 10 mg of PEBP-*b*-PBYP backbone was soaked in the pH 2 sodium hydroxide solution and incubated in the 37°C shaker for 20 weeks. After a clear solution was formed, the solution was adjusted to pH 7.0 and lyophilized into powder before being tested.

3. Cytotoxicity assay. The cytotoxicity assay has been carried out as reported previously[58]. RAW 264.7 (2×10^4 cells/well) mouse macrophages were plated in 96-well plate in Dulbecco's Modified Eagle Medium (DMEM) (10% fetal bovine serum and 1% penicillin/streptomycin). Cells were incubated at 37 °C in a humidified atmosphere containing 5% CO_2 for 24 h to adhere. Then, the medium was replaced with a fresh medium 1-h prior to the addition of 20 μL of the PPE micelles, SCKs and their degradation products, Lipofectamine, PEI and Cremophor-EL to 100 μL of the medium (final concentrations ranged from 0.7–166.7 μg/mL for Lipofectamine and PEI, 20–10,000 μg/mL for Cremophor-EL and 6–3000 μg/mL for PPE formulations). The cells were incubated with the formulations for 24 h and washed once with PBS and 100 μL of the complete media was added to the cells. MTS combined reagent (20 μL) was added to each well (Cell Titer 96® Aqueous Non-Radioactive Cell Proliferation Assay, Promega Co., Madison, WI). The cells were incubated with the reagent for 2 h at 37 °C in a humidified atmosphere containing 5% CO_2 protected from light. Absorbance was measured at 490 nm using SpectraMax M5 (Molecular Devices Co., Sunnyvale, CA). Cell viability was calculated based on the relative absorbance to the control-untreated cells. The calculation of the IC_{50} values and the statistical analysis were performed using GraphPad Prism four-parameter fit, considering the 0% and 100% cell viabilities are for the control medium (no cells) and cells with no treatment, respectively.

4. Multiplex assay. The multiplex assay has been performed as reported previously[58]. The RAW 264.7 cells were treated with medium (control), PPE micelles, SCKs and their degradation products (5 μg/mL) for 24 h. The supernatants were then collected and centrifuged for 10 min at 13,000 rpm. Serial dilutions of cytokine standards were also prepared in the same diluent utilized for the samples (*i.e.* cell-culture medium). Control, standards and nanoparticle-treated samples (50 μL) were incubated with antibody-conjugated magnetic beads for 30 min in the dark. After washing, the detection antibody was added to the wells and incubated in the dark for 30 min under continuous shaking (300 rpm). After washing, streptavidin-phycoerythrin was added to each well and incubated while protected from light for 10 min under the same shaking conditions. Finally, after several washings and re-suspension in the assay buffer and shaking, the expression of the mouse cytokines, interleukin (IL)-1α, IL-1β, IL-2, IL-3, IL-4, IL-5, IL-6, IL-9, IL-10, IL-12 (P40), IL-12 (P70), IL-13, IL-17, Eotaxin, granulocyte-colony-stimulating factor (G-CSF), granulocyte macrophage-colony-stimulating factor (GM-CSF), interferon-γ (IFN-γ), keratinocyte-derived chemokine (KC), monocyte chemotactic protein (MCP)-1, macrophage inflammatory protein (MIP)-1α, MIP-1β, regulated upon activation normal T-cell expressed and presumably secreted (RANTES) and tumor necrosis factor-α (TNF-α) was measured immediately using Bioplex 200 system with HTF and Pro II Wash station (Bio-Rad Laboratories, Inc., Hercules, CA) and the data was analyzed using the Bioplex Data Pro software.

5. Protein adsorption assay. Adsorption of the mouse cytokines, IL-1α, IL-1β, IL-2, IL-3, IL-4, IL-5, IL-6, IL-9, IL-10, IL-12 (P40), IL-12 (P70), IL-13, IL-17, Eotaxin, G-CSF, GM-CSF, IFN-γ, KC, MCP-1, MIP-1α, MIP-1β, RANTES and TNF-α by PPE micelles and SCKs, was measured using a Bioplex 200 system with HTF and Pro II Wash station. Specific concentrations of the standards of each cytokine were determined either in cell culture medium (the same medium used in the multiplex assay section) or when mixed with the various nanoparticles (500 μg/mL) in the same medium, as has been described in the previous section. The values are presented as the ratio of the cytokines in the cytokines/nanoparticles mixture to the solution that contains the same amount of the cytokines but without the nanoparticles.

6. Endotoxin assay. The endotoxin contents of the various samples were measured by using the Pierce® Limulus Amebocyte Lysate (LAL) Chromogenic Endotoxin Quantitation Kit, according to the manufacturer instructions and as described previously[14]. Briefly, all reagents were equilibrated to the room temperature, while the 96-well microplate was maintained at 37°C. To each well, 50 μL of each endotoxin standards, blank (endotoxin-free water), PPE micelles, SCKs and their degradation products was dispensed and the plate was covered and incubated for 5 min at 37°C. Then, 50 μL of LAL was added to each well, gently agitated for 10 seconds and incubated again for 10 min at 37°C, followed by the addition of 100 μL of substrate solution. After gentle agitation and incubation for 6 min at 37°C, 50 μL of 25% acetic acid (stop reagent) was added to each well and the absorbance was measured at 405 nm using SpectraMax M5. The concentration of endotoxin in the standards and samples was determined after constructing a standard curve from the corrected absorbance values.

7. Statistical analysis. Values are presented as mean ± SD of at least three independent experiments. Significance of the differences between two groups was evaluated by Student's t test (unpaired) or between more than two groups by one-way ANOVA followed by Tukey's multiple comparison tests. Differences between different groups were considered significant for p values less than 0.05.

1. Perry, J. L., Herlihy, K. P., Napier, M. E. & Desimone, J. M. PRINT: a novel platform toward shape and size specific nanoparticle theranostics. *Acc. Chem. Res.* **44**, 990–998 (2011).
2. von Maltzahn, G. *et al.* Nanoparticles that communicate in vivo to amplify tumour targeting. *Nat. Mater.* **10**, 545–552 (2011).
3. Elsabahy, M. & Wooley, K. L. Design of polymeric nanoparticles for biomedical delivery applications. *Chem. Soc. Rev.* **41**, 2545–2561 (2012).
4. Rolland, J. *et al.* Polyelectrolyte complex nanoparticles from chitosan and poly(acrylic acid) and Polystyrene-block-poly(acrylic acid). *J. Polym. Sci. Part A: Polym. Chem.* **50**, 4484–4493 (2012).
5. Dobrovolskaia, M. A. & McNeil, S. E. Immunological properties of engineered nanomaterials. *Nat. Nanotechnol.* **2**, 469–478 (2007).
6. Aggarwal, P., Hall, J. B., McLeland, C. B., Dobrovolskaia, M. A. & McNeil, S. E. Nanoparticle interaction with plasma proteins as it relates to particle biodistribution, biocompatibility and therapeutic efficacy. *Adv. Drug Deliv. Rev.* **61**, 428–437 (2009).

7. Samarajeewa, S., Shrestha, R., Li, Y. & Wooley, K. L. Degradability of poly(Lactic Acid)-containing nanoparticles: Enzymatic access through a cross-linked shell barrier. *J. Am. Chem. Soc.* **134**, 1235–1242 (2012).
8. Samarajeewa, S. *et al*. In vitro efficacy of paclitaxel-loaded dual-responsive shell cross-linked polymer nanoparticles having orthogonally degradable disulfide cross-linked corona and polyester core domains. *Mol. Pharm.* **10**, 1092–1099 (2013).
9. Elsabahy, M. & Wooley, K. L. Cytokines as biomarkers of nanoparticle immunotoxicity. *Chem. Soc. Rev.* **42**, 5552–5576 (2013).
10. Deng, Z. J., Liang, M., Monteiro, M., Toth, I. & Minchin, R. F. Nanoparticle-induced unfolding of fibrinogen promotes Mac-1 receptor activation and inflammation. *Nat. Nanotechnol.* **6**, 39–44 (2011).
11. Tan, Y., Li, S., Pitt, B. R. & Huang, L. The inhibitory role of CpG immunostimulatory motifs in cationic lipid vector-mediated transgene expression in vivo. *Hum. Gene. Ther.* **10**, 2153–2161 (1999).
12. Elsabahy, M. & Wooley, K. L. Strategies toward well-defined polymer nanoparticles inspired by nature: chemistry versus versatility. *J. Polym. Sci. Part A: Polym. Chem.* **50**, 1869–1880 (2012).
13. Klyachko, N. L. *et al.* Cross-linked antioxidant nanozymes for improved delivery to CNS. *Nanomedicine* **8**, 119–129 (2012).
14. Elsabahy, M., Samarajeewa, S., Raymond, J. E., Clark, C. & Wooley, K. L. Shell-crosslinked knedel-like nanoparticles induce lower immunotoxicity than their non-crosslinked analogs. *J. Mater. Chem. B* **1**, 5241–5255 (2013).
15. Silvers, A. L., Chang, C. C. & Emrick, T. Functional aliphatic polyesters and nanoparticles prepared by organocatalysis and orthogonal grafting chemistry. *J. Polym. Sci. Part A: Polym. Chem.* **50**, 3517–3529 (2012).
16. Tan, J. H. *et al.* Hyperbranched polymers as delivery vectors for oligonucleotides. *J. Polym. Sci. Part A: Polym. Chem.* **50**, 2585–2595 (2012).
17. Zhang, S. *et al.* Rapid and versatile construction of diverse and functional nanostructures derived from a polyphosphoester-based biomimetic block copolymer system. *J. Am. Chem. Soc.* **134**, 18467–18474 (2012).
18. Shen, Y. *et al.* Polyphosphoester-based cationic nanoparticles serendipitously release integral biologically-active components to serve as novel degradable inducible nitric oxide synthase inhibitors. *Adv. Mater.* **25**, 5609–5614 (2013).
19. Zhang, S., Li, A., Zou, J., Lin, L. Y. & Wooley, K. L. Facile synthesis of clickable, water-soluble and degradable polyphosphoesters. *ACS Macro Lett.* **1**, 328–333 (2012).
20. Hunt, J. N. *et al.* Tunable, high modulus hydrogels driven by ionic coacervation. *Adv. Mater.* **23**, 2327–2331 (2011).
21. Baran, J. & Penczek, S. Hydrolysis of polyesters of phosphoric-acid. 1. kinetics and the pH profile. *Macromolecules* **28**, 5167–5176 (1995).
22. Yang, X.-Z., Wang, Y.-C., Tang, L.-Y., Xia, H. & Wang, J. Synthesis and characterization of amphiphilic block copolymer of polyphosphoester and poly(L-lactic acid). *J. Polym. Sci. Part A: Polym. Chem.* **46**, 6425–6434 (2008).
23. Liu, J. *et al.* Hyperbranched polyphosphates for drug delivery application: design, synthesis, and in vitro evaluation. *Biomacromolecules* **11**, 1564–1570 (2010).
24. Wang, Y.-C., Tang, L.-Y., Li, Y. & Wang, J. Thermoresponsive block copolymers of poly(ethylene glycol) and polyphosphoester: thermo-induced self-assembly, biocompatibility, and hydrolytic degradation. *Biomacromolecules* **10**, 66–73 (2008).
25. Iwasaki, Y. & Akiyoshi, K. Design of biodegradable amphiphilic polymers: well-defined amphiphilic polyphosphates with hydrophilic graft chains via ATRP. *Macromolecules* **37**, 7637–7642 (2004).
26. Iwasaki, Y., Nakagawa, C., Ohtomi, M., Ishihara, K. & Akiyoshi, K. Novel biodegradable polyphosphate cross-linker for making biocompatible hydrogel. *Biomacromolecules* **5**, 1110–1115 (2004).
27. He, J. *et al.* Synthesis and physicochemical characterization of biodegradable and pH-responsive hydrogels based on polyphosphoester for protein delivery. *J. Polym. Sci. Part A: Polym. Chem.* **48**, 1919–1930 (2010).
28. Du, J.-Z., Sun, T.-M., Weng, S.-Q., Chen, X.-S. & Wang, J. Synthesis and characterization of photo-cross-linked hydrogels based on biodegradable polyphosphoesters and poly(ethylene glycol) copolymers. *Biomacromolecules* **8**, 3375–3381 (2007).
29. Wang, J., Mao, H.-Q. & Leong, K. W. A novel biodegradable gene carrier based on polyphosphoester. *J. Am. Chem. Soc.* **123**, 9480–9481 (2001).
30. Lu, Z.-Z. *et al.* Biodegradable polycation and plasmid DNA multilayer film for prolonged gene delivery to mouse osteoblasts. *Biomaterials* **29**, 733–741 (2008).
31. Du, J.-Z. *et al.* Synthesis and micellization of amphiphilic brush-coil block copolymer based on poly(ε-caprolactone) and PEGylated polyphosphoester. *Biomacromolecules* **7**, 1898–1903 (2006).
32. Wang, Y.-C. *et al.* Self-assembled micelles of biodegradable triblock copolymers based on poly(ethyl ethylene phosphate) and poly(ϵ-caprolactone) as drug carriers. *Biomacromolecules* **9**, 388–395 (2007).
33. Wachiralarpphaithoon, C., Iwasaki, Y. & Akiyoshi, K. Enzyme-degradable phosphorylcholine porous hydrogels cross-linked with polyphosphoesters for cell matrices. *Biomaterials* **28**, 984–993 (2007).
34. Shao, H., Zhang, M., He, J. & Ni, P. Synthesis and characterization of amphiphilic poly(ε-caprolactone)-b-polyphosphoester diblock copolymers bearing multifunctional pendant groups. *Polymer* **53**, 2854–2863 (2012).
35. Wang, Y.-C. *et al.* Engineering nanoscopic hydrogels via photo-crosslinking salt-induced polymer assembly for targeted drug delivery. *Chem. Commun.* **46**, 3520–3522 (2010).
36. Xiong, M.-H. *et al.* Synthesis of PEG-armed and polyphosphoester core-cross-linked nanogel by one-step ring-opening polymerization. *Macromolecules* **42**, 893–896 (2009).
37. Xiong, M.-H. *et al.* Bacteria-responsive multifunctional nanogel for targeted antibiotic delivery. *Adv. Mater.* **24**, 6175–6180 (2012).
38. Zou, J. *et al.* pH-Triggered reversible morphological inversion of orthogonally-addressable poly(3-acrylamidophenylboronic acid)-block-poly(acrylamidoethylamine) micelles and their shell crosslinked nanoparticles. *J. Polym. Sci. Part A: Polym. Chem.* **3**, 3146–3156 (2012).
39. Samarajeewa, S. *et al.* Degradable cationic shell cross-linked knedel-like nanoparticles: Synthesis, degradation, nucleic acid binding, and in vitro evaluation. *Biomacromolecules* **14**, 1018–1027 (2013).
40. Elsabahy, M. *et al.* Multifunctional hierarchically assembled nanostructures as complex stage-wise dual-delivery systems for coincidental yet differential trafficking of siRNA and paclitaxel. *Nano Lett.* **13**, 2172–2181 (2013).
41. Huang, S. J., Wang, T. P., Lue, S. I. & Wang, L. F. Pentablock copolymers of pluronic F127 and modified poly(2-dimethyl amino)ethyl methacrylate for internalization mechanism and gene transfection studies. *Int. J. Nanomedicine* **8**, 2011–2027 (2013).
42. Zhang, G., Liu, J., Yang, Q., Zhuo, R. & Jiang, X. Disulfide-containing brushed polyethylenimine derivative synthesized by click chemistry for nonviral gene delivery. *Bioconjug. Chem.* **23**, 1290–1299 (2012).
43. Val, S. *et al.* Carbon black and titanium dioxide nanoparticles induce pro-inflammatory responses in bronchial epithelial cells: need for multiparametric evaluation due to adsorption artifacts. *Inhal. Toxicol.* **21**, 115–122 (2009).
44. Kocbach, A., Totlandsdal, A. I., Lag, M., Refsnes, M. & Schwarze, P. E. Differential binding of cytokines to environmentally relevant particles: a possible source for misinterpretation of in vitro results? *Toxicol. Lett.* **176**, 131–137 (2008).
45. Li, A. *et al.* Synthesis and in vivo pharmacokinetic evaluation of degradable shell cross-linked polymer nanoparticles with poly(carboxybetaine) versus poly(ethylene glycol) surface-grafted coatings. *ACS Nano* **6**, 8970–8982 (2012).
46. Keefe, A. J. & Jiang, S. Poly(zwitterionic)protein conjugates offer increased stability without sacrificing binding affinity or bioactivity. *Nature Chem.* **4**, 59–63 (2012).
47. Rodriguez-Emmenegger, C. *et al.* Polymer brushes showing non-fouling in blood plasma challenge the currently accepted design of protein resistant surfaces. *Macromol. Rapid Commun.* **32**, 952–957 (2011).
48. Jiang, S. & Cao, Z. Ultralow-fouling, functionalizable, and hydrolyzable zwitterionic materials and their derivatives for biological applications. *Adv. Mater.* **22**, 920–932 (2010).
49. Elsabahy, M. *et al.* Differential immunotoxicities of poly(ethylene glycol)- *vs.* poly(carboxybetaine)-coated nanoparticles. *J. Control. Release* 10.1016/j.jconrel.2013.1009.1010 (2013).
50. Deng, Z. J., Liang, M., Toth, I., Monteiro, M. & Minchin, R. F. Plasma protein binding of positively and negatively charged polymer-coated gold nanoparticles elicits different biological responses. *Nanotoxicology* **7**, 314–322 (2013).
51. Benjamini, E., Coico, R. & Sunshine, G. in Immunology (ed. Margulies, D. H.) (John Wiley & Sons, Inc., New York, 2000).
52. Zhang, L. W., Yu, W. W., Colvin, V. L. & Monteiro-Riviere, N. A. Biological interactions of quantum dot nanoparticles in skin and in human epidermal keratinocytes. *Toxicol. Appl. Pharmacol.* **228**, 200–211 (2008).
53. Ryman-Rasmussen, J. P., Riviere, J. E. & Monteiro-Riviere, N. A. Surface coatings determine cytotoxicity and irritation potential of quantum dot nanoparticles in epidermal keratinocytes. *J. Invest. Dermatol.* **127**, 143–153 (2007).
54. Beyerle, A., Irmler, M., Beckers, J., Kissel, T. & Stoeger, T. Toxicity pathway focused gene expression profiling of PEI-based polymers for pulmonary applications. *Mol. Pharm.* **7**, 727–737 (2010).
55. Powers, M. R., Davies, M. H. & Eubanks, J. P. Increased expression of chemokine KC, an interleukin-8 homologue, in a model of oxygen-induced retinopathy. *Curr. Eye Res.* **30**, 299–307 (2005).
56. Kim, B. H., Lee, Y. S. & Kang, K. S. The mechanism of retinol-induced irritation and its application to anti-irritant development. *Toxicol. Lett.* **146**, 65–73 (2003).
57. Cubillos-Ruiz, J. R. *et al.* Polyethylenimine-based siRNA nanocomplexes reprogram tumor-associated dendritic cells via TLR5 to elicit therapeutic antitumor immunity. *J. Clin. Invest.* **119**, 2231–2244 (2009).
58. Shrestha, R., Elsabahy, M., Florez-Malaver, S., Samarajeewa, S. & Wooley, K. L. Endosomal escape and siRNA delivery with cationic shell crosslinked knedel-like nanoparticles with tunable buffering capacities. *Biomaterials* **33**, 8557–8568 (2012).
59. Shah, P. N. *et al.* Synthesis, characterization, and in vivo efficacy of shell cross-linked nanoparticle formulations carrying silver antimicrobials as aerosolized therapeutics. *ACS Nano* **7**, 4977–4987 (2013).
60. Ibricevic, A. *et al.* PEGylation of cationic, shell-crosslinked-knedel-like nanoparticles modulates inflammation and enhances cellular uptake in the lung. *Nanomedicine doi: 10.1016/j.nano.2013.02.006* (2013).

Acknowledgments

We gratefully acknowledge financial support from the National Heart Lung and Blood Institute of the National Institutes of Health as a Program of Excellence in Nanotechnology (HHSN268201000046C), the National Institute of Diabetes and Digestive and Kidney

Diseases of the National Institutes of Health (R01-DK082546), and the National Science Foundation under grant number DMR-0906815 and DMR-1105304. The Welch Foundation is gratefully acknowledged for support through the W. T. Doherty-Welch Chair in Chemistry, Grant No. A-0001. The transmission electron microscopy facilities at Washington University in St. Louis, Department of Otolaryngology, and Research Center for Auditory and Visual Studies funded by NIH P30 DC004665 are gratefully acknowledged. ZJD acknowledges a Fellowship support from the NHMRC. PTH acknowledges support as David H. Koch Chair.

Author contributions

M.E. and S.Z. designed the project, performed the experiments and wrote the manuscript. F.Z., Y.H.L., H.W. and P.P. helped out with the experiments. Z.J.D. and P.T.H. participated in the analysis and discussion of the results and in writing the manuscript. K.L.W. designed the study, wrote the manuscript and supervised the project. All authors reviewed the manuscript.

Additional information

Supplementary information accompanies this paper at http://www.nature.com/scientificreports

Competing financial interests: The authors declare no competing financial interests.

How to cite this article: Elsabahy, M. *et al*. Surface Charges and Shell Crosslinks Each Play Significant Roles in Mediating Degradation, Biofouling, Cytotoxicity and Immunotoxicity for Polyphosphoester-based Nanoparticles. *Sci. Rep.* **3**, 3313; DOI:10.1038/srep03313 (2013).